

Cite as: D. Notz and J. Stroeve,  
*Science* 10.1126/science.aag2345  
(2016).

# Observed Arctic sea-ice loss directly follows anthropogenic CO<sub>2</sub> emission

Dirk Notz<sup>1\*</sup> and Julienne Stroeve<sup>2,3</sup>

<sup>1</sup>Max-Planck-Institute for Meteorology, Hamburg, Germany. <sup>2</sup>National Snow and Ice Data Center, Boulder, CO, USA. <sup>3</sup>University College, London, UK.

\*Corresponding author. E-mail: dirk.notz@mpimet.mpg.de

Arctic sea ice is retreating rapidly, raising prospects of a future ice-free Arctic Ocean during summer. Since climate-model simulations of the sea-ice loss differ substantially, we here use a robust linear relationship between monthly-mean September sea-ice area and cumulative CO<sub>2</sub> emissions to infer the future evolution of Arctic summer sea ice directly from the observational record. The observed linear relationship implies a sustained loss of  $3 \pm 0.3$  m<sup>2</sup> of September sea-ice area per metric ton of CO<sub>2</sub> emission. Based on this sensitivity, Arctic sea-ice will be lost throughout September for an additional 1000 Gt of CO<sub>2</sub> emissions. Most models show a lower sensitivity, which is possibly linked to an underestimation of the modeled increase in incoming longwave radiation and of the modeled Transient Climate Response.

The ongoing rapid loss of Arctic sea ice has far reaching consequences for climate, ecology, and human activities alike. These include amplified warming of the Arctic (1), possible linkages of sea-ice loss to mid-latitude weather patterns (2), changing habitat for flora and fauna (3), and changing prospects for human activities in the high North (3). To understand and manage these consequences and their possible future manifestation, we need to understand the sensitivity of Arctic sea-ice evolution to changes in the prevailing climate conditions. However, assessing this sensitivity has been challenging. For example, climate-model simulations differ widely in their timing of the loss of Arctic sea ice for a given trajectory of anthropogenic CO<sub>2</sub> emissions: While in the most recent Climate Model Intercomparison Project 5 (CMIP5) (4) some models project a near ice-free Arctic during the summer minimum already toward the beginning of this century, other models keep a substantial amount of ice well into the next century even for an external forcing based on largely undamped anthropogenic CO<sub>2</sub> emissions as described by the Representative Concentration Pathway scenario RCP8.5 (4, 5).

To robustly estimate the sensitivity of Arctic sea ice to changes in the external forcing, we here identify and examine a fundamental relationship in which the CMIP5 models agree with the observational record: during the transition to a seasonally ice-free Arctic Ocean, the 30-year running mean of monthly mean September Arctic sea-ice area is almost linearly related to cumulative anthropogenic CO<sub>2</sub> emissions (Fig. 1). In the model simulations, the linear relationship holds until the 30-year running mean, which we analyze to reduce internal variability, samples more and more years of a seasonally ice-free Arctic Ocean, at which point the rela-

tionship levels off toward zero. For the first few decades of the simulations, a few models simulate a near-constant sea-ice cover despite slightly rising cumulative CO<sub>2</sub> emissions. This suggests that in these all-forcing simulations, greenhouse-gas emissions were initially not the dominant driver of sea-ice evolution. This notion is confirmed by the CMIP5 1% CO<sub>2</sub> simulations, where the initial near-constant sea-ice cover does not occur (fig. S3A). With rising greenhouse-gas emissions, the impact of CO<sub>2</sub> becomes dominating also in all all-forcing simulations, as evident by the robust linear trend that holds in all simulations throughout the transition period to seasonally ice-free conditions. We define this transition period to start when the 30-year mean September Arctic sea-ice area in a particular simulation decreases for the first time to an area that is 10% or more below the simulation's minimum sea-ice cover during the period 1850–1900, and to end once the 30-year mean September Arctic sea-ice area drops for the first time below 1 million km<sup>2</sup> (see table S1 for specific numbers).

The existence of a robust, linear relationship between cumulative CO<sub>2</sub> emissions and Arctic sea-ice area in all CMIP5 models and in the observational record extends the findings of earlier studies that demonstrated such relationships for individual, sometimes more simplified models (6, 7), and of studies that have demonstrated a linear relationship between Arctic sea-ice area and either global mean temperature (5, 8–12) or atmospheric CO<sub>2</sub> concentration (13, 14). These linear relationships are highly suggestive of a fundamental underlying mechanism, which has been elusive so far. We will later suggest a conceptual explanation of the linearity, but before doing so we first discuss two implications of the observed linear relationship that are independ-

ent of its underlying mechanism.

First, the observed linear relationship allows us to estimate a sensitivity of  $3.0 \pm 0.1 \text{ m}^2$  of September Arctic sea-ice loss per ton of anthropogenic  $\text{CO}_2$  emissions during the observational period 1953–2015. This number is sufficiently intuitive to allow one to grasp the contribution of personal  $\text{CO}_2$  emissions to the loss of Arctic sea ice. For example, based on the observed sensitivity, the average personal  $\text{CO}_2$  emissions of several metric tons per year can be directly linked to the loss of tens of  $\text{m}^2$  of Arctic sea ice every single year (see fig. S1).

Second, the linear relationship allows for a robust evaluation of climate-model simulations. While a number of previous studies have found that the observed sea-ice retreat has been faster than projected by most climate-model simulations (15, 16), it has remained unclear whether these differences are primarily a manifestation of internal variability (17, 18). The sensitivity that we estimate here is, in contrast, based on the average evolution over many decades, thus eliminating internal variability to a substantial degree. A mismatch between the observed and the simulated sensitivity hence robustly indicates a shortcoming either in the model or in the external forcing fields used for a simulation.

Evaluating the simulated sensitivity, we find that most CMIP5 models systematically underestimate the observed sensitivity of Arctic sea ice relative to anthropogenic  $\text{CO}_2$  emissions of  $3.0 \pm 0.3 \text{ m}^2$  (see table S1 for details). Across the full transition range to near ice-free conditions, the multimodel mean sensitivity is only  $1.75 \pm 0.67 \text{ m}^2$  loss of Arctic sea ice per metric ton of anthropogenic  $\text{CO}_2$  emissions. Because of the linear response, a similar sensitivity is obtained for subperiods of the transition period that have the same length as our observational record, with overall maximum sensitivities over such 61-year-long time periods from individual simulations of  $1.95 \pm 0.70 \text{ m}^2/\text{ton}$ . Note that these estimates of the models' sensitivity might be biased somewhat high, as previous studies found that the aerosol forcing of CMIP5 simulations might have been too weak in recent decades (19, 20). This would give rise to artificially amplified warming and thus amplified sea-ice loss in these simulations, rendering the true sensitivity of the models to be even lower than the values we estimate here.

The low sensitivity of the modeled sea-ice response can be understood through a conceptual model that explains the linearity. To derive such a conceptual model, we consider the annual mean surface energy balance at the ice edge, which describes the fact that the net incoming shortwave radiation  $(1-\alpha)F_{sw}$  and the incoming non-shortwave flux  $F_{nonSW,in}$  are balanced by the outgoing non-shortwave flux and the conductive heat flux at the surface of the ice.

With increasing atmospheric  $\text{CO}_2$  concentration, the incoming non-shortwave flux increases at the ice edge in re-

sponse to the rising atmospheric emissivity and related atmospheric feedbacks. However, neither the outgoing non-shortwave flux nor the conductive heat flux in the ice will change much, as the surface properties of sea ice at the ice edge are largely independent of its location. We conjecture that this also holds for total albedo  $\alpha$ , since a possible rise in cloudiness caused by sea-ice loss (21) will primarily occur over the open water south of the moving ice edge, rather than at the ice edge itself. In addition, the albedo of clouds is comparable to that of the ice at the ice edge. Hence, it seems plausible to assume that the surface energy balance at the ice edge is primarily kept closed by a decrease in the incoming shortwave flux that compensates for the increase in incoming non-shortwave flux. Such decrease of the incoming shortwave radiation is obtained by the northward movement of the ice edge to a region with less annual mean solar irradiance. Equilibrium is re-established at the ice edge when

$$\Delta F_{sw}(1-\alpha) = -\Delta F_{nonSW,in}. \quad (1)$$

If we now for simplicity assume a circular shape of the sea-ice cover centered at the North Pole, the sea-ice area that is enclosed by any given latitude has virtually the same latitudinal dependence as the annual mean incoming shortwave radiation at the top of the atmosphere (Fig. 2A). Hence, the change in area enclosed by the ice edge  $\Delta A_{seaice}$  should roughly be proportional to the change in incoming annual mean shortwave radiation at the ice edge (Fig. 2B),

$$\Delta A_{seaice} \propto \Delta F_{sw}(1-\alpha) \quad (2)$$

We additionally find empirically that the incoming non-shortwave flux is fairly linearly related to anthropogenic  $\text{CO}_2$  emissions  $E_{CO_2}$  across CMIP5 model simulations both in the Arctic, where the loss of sea-ice might amplify the change in radiative forcing, and globally, where such amplification is small (fig. S2). This linearity arises because more of each ton of emitted  $\text{CO}_2$  remains in the atmosphere as oceanic  $\text{CO}_2$  uptake decreases in the future. This then roughly compensates for the logarithmic rather than linear change of atmospheric long-wave emission with changes in atmospheric  $\text{CO}_2$  concentration (22). It is hence a plausible assumption that the linearity of incoming long-wave radiation with rising  $\text{CO}_2$  emissions also holds at the ice edge, and we can write

$$\Delta F_{nonSW,in} = \frac{dF_{nonSW,in}}{dE_{CO_2}} \Delta E_{CO_2} \quad (3)$$

Inserting Eqs. (2) and (3) into Eq. (1) then finally gives

$$\Delta A_{\text{seai ce}} = \frac{dF_{\text{nonSW,in}}}{dE_{\text{CO}_2}} \Delta E_{\text{CO}_2} \quad (4)$$

which for constant  $dF_{\text{nonSW,in}}/dE_{\text{CO}_2}$  is a possible explanation for the observed linear relationship between Arctic sea-ice area and cumulative CO<sub>2</sub> emission.

Based on this expression, we can infer that most climate models underestimate the loss of Arctic sea ice because they underestimate the increase of incoming non-shortwave flux for a given increase of anthropogenic CO<sub>2</sub> emissions. An analysis of the available fields of surface heat fluxes in the CMIP5 archive confirms this notion, with high correlation between modeled sea-ice sensitivity and modeled changes in either incoming total non-shortwave flux or incoming longwave radiation, as the latter dominates the change in the non-shortwave flux (Fig. 3, A to D). Unfortunately, observational uncertainty is currently too large to test our finding of too low an increase in incoming longwave radiation against independent records (23).

On a more regional scale, our conceptual explanation allows us to ascribe a minor role for the overall evolution of sea ice to processes that are unrelated to the large-scale change in atmospheric forcing. This includes a minor role of oceanic heat transport on the time scales that we consider here, since we can derive a linear relationship without considering these transports. While it might alternatively be possible that the oceanic heat transports have changed monotonously in recent decades, we have no indication that this is the case from either observations or model simulations. The current minor role of oceanic heat transports implies that on time scales of several centuries, the linearity will most likely no longer hold, since sensitivity will increase once changes in oceanic heat content start measurably affecting Arctic sea-ice coverage (12).

Our results also suggest that regional differences in atmospheric heat-flux convergence or wind forcing do not significantly affect the Arctic-wide mean energy balance on the time scales that we consider here. On the other hand this also explains why the linear relationship does not hold in the Antarctic, where dynamical forcing from wind and oceanic heat transport are key drivers of the large-scale sea-ice evolution.

The apparent minor role of oceanic heat transport, and the correlation between the change in global surface fluxes and Arctic sea-ice loss, suggest that we can use the observed evolution of Arctic sea ice as an emergent constraint on Transient Climate Response (TCR). This is commonly defined as the global-mean warming at the time of doubled atmospheric CO<sub>2</sub> concentration following a 1% CO<sub>2</sub> increase

per year (24). Indeed, we find good correlation between the modeled sea-ice sensitivity and TCR both in the full-forcing simulations (Fig. 3E) and in the simulations with rising CO<sub>2</sub> only (fig. S3B).

Unfortunately, while indicative of a TCR at the higher end of simulated values, the correlation does not allow for a direct estimate of TCR for two reasons: First, the loss of Arctic sea ice is more directly driven by the regional temperature rise in the Arctic rather than the global temperature rise that is expressed by the TCR. Any failure of the models to realistically simulate the ratio between global and Arctic temperature rise, usually referred to as Arctic Amplification, could hence lead to an erroneous quantitative estimate of the TCR based on the correlation that we identify. Second, TCR is estimated from simulations where all non-CO<sub>2</sub> forcings are kept constant, while the non-CO<sub>2</sub> forcings change in the historical and RCP8.5 simulations that we consider here. This affects at least to some degree the robustness of the correlation (see Supplementary Text for details.)

Previous studies that estimated climate sensitivity from emergent constraints have usually focused on the Equilibrium Climate Sensitivity (ECS), which describes the equilibrium global-mean warming for a sustained doubling of atmospheric CO<sub>2</sub> concentration. They also come to the conclusion that the real sensitivity of the Earth climate system is at the higher end of simulated values, either from analyzing atmospheric convective mixing (25) or mid-troposphere relative humidity (26). In contrast, studies analyzing the Earth's energy budget, in particular after considering the recent slowing down in atmospheric warming, find that the TCR should be at the lower end of simulated values (27, 28). This result, however, might be biased by the different data coverage in models and observations (29).

Regarding the future evolution of sea ice, our analysis suggests that there is little reason to believe that the observed sensitivity of Arctic sea-ice loss will change substantially in the foreseeable future. Hence, we can directly estimate that the remainder of Arctic summer sea ice will be lost for roughly an additional 1000 Gt of CO<sub>2</sub> emissions based on the observed sensitivity of  $3.0 \pm 0.3 \text{ m}^2$  September sea-ice loss per ton of anthropogenic CO<sub>2</sub> emissions. Since this estimate is based on the 30-year running mean of monthly averages, it is a very conservative estimate of the cumulative emissions at which the annual minimum sea-ice area drops below 1 million km<sup>2</sup> for the first time. In addition, internal variability causes an uncertainty of around 20 years as to the first year of a near-complete loss of Arctic sea ice (18, 30). For current emissions of 35 Gt CO<sub>2</sub> per year, the limit of 1000 Gt will be reached before mid century. On the other hand, our results also imply that any measure taken to mitigate CO<sub>2</sub> emissions will directly slow down the ongoing loss of Arctic summer sea ice. In particular, for cumulative



future total emissions compatible with reaching a 1.5°C global warming target, i.e., for cumulative future emissions significantly below 1000 Gt, Arctic summer sea ice has a chance of long-term survival at least in some parts of the Arctic Ocean.

## REFERENCES AND NOTES

1. F. Pithan, T. Mauritsen, Arctic amplification dominated by temperature feedbacks in contemporary climate models. *Nat. Geosci.* **7**, 181–184 (2014). doi:10.1038/ngeo2071
2. T. Vihma, Effects of Arctic sea ice decline on weather and climate: A review. *Surv. Geophys.* **35**, 1175–1214 (2014). doi:10.1007/s10712-014-9284-0
3. W. N. Meier, G. K. Hovelsrud, B. E. H. van Oort, J. R. Key, K. M. Kovacs, C. Michel, C. Haas, M. A. Granskog, S. Gerland, D. K. Perovich, A. Makshtas, J. D. Reist, Arctic sea ice in transformation: A review of recent observed changes and impacts on biology and human activity. *Rev. Geophys.* **52**, 185–217 (2014). doi:10.1002/2013RG000431
4. K. E. Taylor, R. J. Stouffer, G. A. Meehl, An overview of CMIP5 and the experiment design. *Bull. Am. Meteorol. Soc.* **93**, 485–498 (2012). doi:10.1175/BAMS-D-11-00094.1
5. J. Stroeve, D. Notz, Insights on past and future sea-ice evolution from combining observations and models. *Global Planet. Change* **135**, 119–132 (2015). doi:10.1016/j.gloplacha.2015.10.011
6. K. Zickfeld, V. K. Arora, N. P. Gillett, Is the climate response to CO<sub>2</sub> emissions path dependent? *Geophys. Res. Lett.* **39**, L05703 (2012). doi:10.1029/2011GL0150205
7. T. Herrington, K. Zickfeld, Path independence of climate and carbon cycle response over a broad range of cumulative carbon emissions. *Earth Syst. Dyn.* **5**, 409–422 (2014). doi:10.5194/esd-5-409-2014
8. J. M. Gregory, P. A. Stott, D. J. Cresswell, N. A. Rayner, C. Gordon, D. M. H. Sexton, Recent and future changes in Arctic sea ice simulated by the HadCM3 AOGCM. *Geophys. Res. Lett.* **29**, 28-1–28-4 (2002). doi:10.1029/2001GL014575
9. M. Winton, Do Climate Models Underestimate the Sensitivity of Northern Hemisphere Sea Ice Cover? *J. Clim.* **24**, 3924–3934 (2011). doi:10.1175/2011JCLI14146.1
10. I. Mahlstein, R. Knutti, September Arctic sea ice predicted to disappear near 2°C global warming above present. *J. Geophys. Res.* **117**, D06104 (2012). doi:10.1029/2011JD016709
11. J. K. Ridley, J. A. Lowe, H. T. Hewitt, How reversible is sea ice loss? *Cryosphere* **6**, 193–198 (2012). doi:10.5194/tc-6-193-2012
12. C. Li, D. Notz, S. Tietsche, J. Marotzke, The Transient versus the equilibrium response of sea ice to global warming. *J. Clim.* **26**, 5624–5636 (2013). doi:10.1175/JCLI-D-12-00492.1
13. O. Johannessen, *Atmos. Ocean. Sci. Lett.* **1**, 51 (2008).
14. D. Notz, J. Marotzke, Observations reveal external driver for Arctic sea-ice retreat. *Geophys. Res. Lett.* **39**, L051094 (2012). doi:10.1029/2012GL051094
15. F. Massonnet, T. Fichefet, H. Goosse, C. M. Bitz, G. Philippon-Berthier, M. M. Holland, P.-Y. Barriat, Constraining projections of summer Arctic sea ice. *Cryosphere* **6**, 1383–1394 (2012). doi:10.5194/tc-6-1383-2012
16. J. C. Stroeve, V. Kattsov, A. Barrett, M. Serreze, T. Pavlova, M. Holland, W. N. Meier, Trends in Arctic sea ice extent from CMIP5, CMIP3 and observations. *Geophys. Res. Lett.* **39**, L16502 (2012). doi:10.1029/2012GL052676
17. G. Flato *et al.*, in *Climate Change 2013: The Physical Science Basis. Contribution of Working Group I to the Fifth Assessment Report of the Intergovernmental Panel on Climate Change*, T. Stocker *et al.*, Eds. (Cambridge Univ. Press, 2013), chap. 9, pp. 741–866.
18. D. Notz, How well must climate models agree with observations? *Philos. Trans. R. Soc. A* **373**, 20140164 (2015). doi:10.1098/rsta.2014.0164 Medline
19. B. D. Santer, C. Bonfils, J. F. Painter, M. D. Zelinka, C. Mears, S. Solomon, G. A. Schmidt, J. C. Fyfe, J. N. S. Cole, L. Nazarenko, K. E. Taylor, F. J. Wentz, Volcanic contribution to decadal changes in tropospheric temperature. *Nat. Geosci.* **7**, 185–189 (2014). doi:10.1038/ngeo2098
20. G. A. Schmidt, D. T. Shindell, K. Tsigaridis, Reconciling warming trends. *Nat. Geosci.* **7**, 158–160 (2014). doi:10.1038/ngeo2105
21. I. V. Gorodetskaya, L.-B. Tremblay, B. Liepert, M. A. Cane, R. I. Cullather, The Influence of Cloud and Surface Properties on the Arctic Ocean shortwave radiation budget in coupled models. *J. Clim.* **21**, 866–882 (2008). doi:10.1175/2007JCLI11614.1
22. H. D. Matthews, N. P. Gillett, P. A. Stott, K. Zickfeld, The proportionality of global warming to cumulative carbon emissions. *Nature* **459**, 829–832 (2009). doi:10.1038/nature08047 Medline
23. G. L. Stephens, J. Li, M. Wild, C. A. Clayson, N. Loeb, S. Kato, T. L'Ecuyer, P. W. Stackhouse, M. Lebsock, T. Andrews, An update on Earth's energy balance in light of the latest global observations. *Nat. Geosci.* **5**, 691–696 (2012). doi:10.1038/ngeo1580
24. U. Cubasch *et al.*, in *Climate Change 2001: The Scientific Basis*, J. T. Houghton *et al.*, Eds. (Cambridge Univ. Press, 2001), chap. 9, pp. 525–582.
25. S. C. Sherwood, S. Bony, J.-L. Dufresne, Spread in model climate sensitivity traced to atmospheric convective mixing. *Nature* **505**, 37–42 (2014). doi:10.1038/nature12829 Medline
26. J. T. Fasullo, K. E. Trenberth, A less cloudy future: The role of subtropical subsidence in climate sensitivity. *Science* **338**, 792–794 (2012). doi:10.1126/science.1227465 Medline
27. A. Otto, F. E. L. Otto, O. Boucher, J. Church, G. Hegerl, P. M. Forster, N. P. Gillett, J. Gregory, G. C. Johnson, R. Knutti, N. Lewis, U. Lohmann, J. Marotzke, G. Myhre, D. Shindell, B. Stevens, M. R. Allen, Energy budget constraints on climate response. *Nat. Geosci.* **6**, 415–416 (2013). doi:10.1038/ngeo1836
28. N. P. Gillett, V. K. Arora, D. Matthews, M. R. Allen, Constraining the ratio of global warming to cumulative CO<sub>2</sub> Emissions using CMIP5 simulations. *J. Clim.* **26**, 6844–6858 (2013). doi:10.1175/JCLI-D-12-00476.1
29. M. Richardson, K. Cowtan, E. Hawkins, M. B. Stolpe, Reconciled climate response estimates from climate models and the energy budget of Earth. *Nat. Clim. Chang.* **6**, 931–935 (2016). doi:10.1038/nclimate3066
30. A. Jahn, J. E. Kay, M. M. Holland, D. M. Hall, How predictable is the timing of a summer ice-free Arctic? *Geophys. Res. Lett.* **43**, 9113–9120 (2016). doi:10.1002/2016GL070067
31. Hadley Center for Climate Prediction and Research, Met Office, HadISST 1.1 - global sea-ice coverage and sea surface temperature (1870-2015); NCAS British Atmospheric Data Centre (2006); <http://badc.nerc.ac.uk/data/hadisst/>.
32. F. Fetterer, K. Knowles, W. Meier, M. Savoie, Sea ice index. *Digital media*, National Snow and Ice Data Center, Boulder, CO (2002, updated 2014).
33. M. Meinshausen, S. J. Smith, K. Calvin, J. S. Daniel, M. L. T. Kainuma, J.-F. Lamarque, K. Matsumoto, S. A. Montzka, S. C. B. Raper, K. Riahi, A. Thomson, G. J. M. Velders, D. P. P. van Vuuren, The RCP greenhouse gas concentrations and their extensions from 1765 to 2300. *Clim. Change* **109**, 213–241 (2011). doi:10.1007/s10584-011-0156-z
34. G. R. North, Theory of energy-balance climate models. *J. Atmos. Sci.* **32**, 2033–2043 (1975). doi:10.1175/1520-0469(1975)032<2033:TOFBCM>2.0.CO;2
35. K. Marvel, G. A. Schmidt, R. L. Miller, L. S. Nazarenko, Implications for climate sensitivity from the response to individual forcings. *Nat. Clim. Chang.* **6**, 386–389 (2016). doi:10.1038/nclimate2888
36. J. M. Gregory, T. Andrews, Variation in climate sensitivity and feedback parameters during the historical period. *Geophys. Res. Lett.* **43**, 3911–3920 (2016). doi:10.1002/2016GL068406
37. European Commission Joint Research Center and PBL Netherlands Environmental Assessment Agency, Emission database for global atmospheric research (EDGAR), release version 4.2, Tech. Rep., European Commission (2014).

## ACKNOWLEDGMENTS

We are very grateful to Jochem Marotzke for his suggestion to analyze the TCR and for very helpful comments on the manuscript. We are also very grateful to two anonymous reviewers, whose insightful comments were essential for framing the final version of our study. We further thank Brian Soden, Dirk Olonscheck and Chao Li for helpful feedback. D.N. acknowledges funding through a Max-Planck Research Fellowship. J.S. acknowledges funding from NASA Grant NNX12AB75G and the National Science Foundation Grant PLR 1304246. All primary data used for this study is based on publically available output from CMIP5 models, and is also available upon request from publications@mpimet.mpg.de.

**SUPPLEMENTARY MATERIALS**

[www.sciencemag.org/cgi/content/full/science.aag2345/DC1](http://www.sciencemag.org/cgi/content/full/science.aag2345/DC1)

[www.sciencemag.org/content/vol/issue/page/suppl/DC1](http://www.sciencemag.org/content/vol/issue/page/suppl/DC1)

Materials and Methods

Supplementary Text

Figs. S1 to S3

Table S1

References (35–37)

27 May 2016; accepted 12 October 2016

Published online 3 November 2016

10.1126/science.aag2345

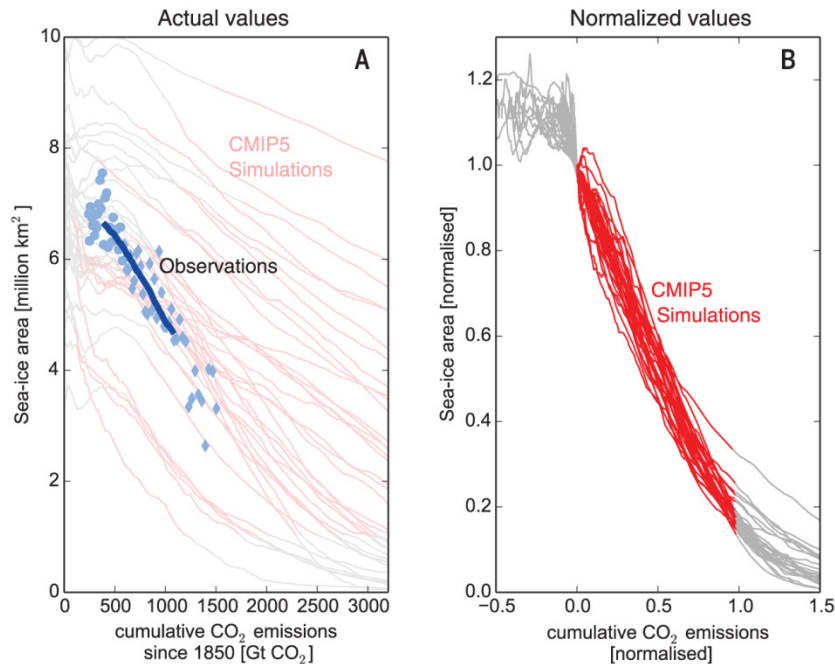


**Fig. 1. Relationship between September Arctic sea-ice area and cumulative anthropogenic CO<sub>2</sub> emissions.** (A) Actual values. The thick blue line shows the 30-year running mean of observed September sea-ice area and the thinner red lines the 30-year running means from CMIP5 model simulations. For reference, we also show the annual values of observed September sea-ice area, based from 1953-1978 on HadISST (31) (circles) and from 1979 to 2015 on the NSIDC sea-ice index (32) (diamonds; see methods for details). (B) Normalised simulations. For this plot, the simulated CMIP5 sea ice-area is normalized by dividing by the simulated sea ice-area at the onset of the transition period as defined in the text. For each simulation, the cumulative emissions (33) are set to 0 at the onset of the transition period and then linearly scaled to reach 1 by the end of the transition period (compare table S1 for actual values). Note that this linearization is only carried out to more explicitly visualize the linearity in the models. All analyses in the paper are based on the original data shown in panel A.

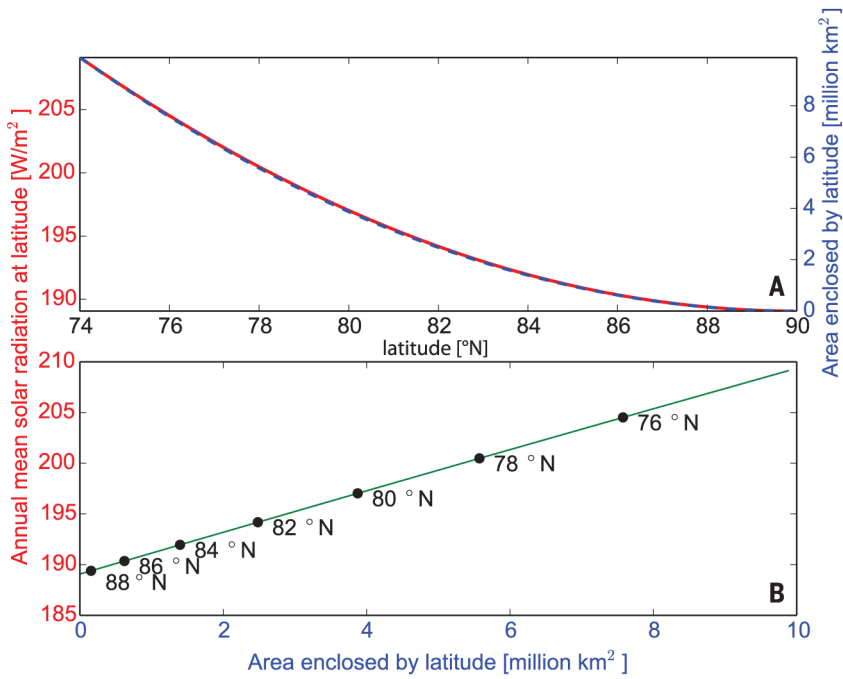


**Fig. 2. Relationship between annual mean incoming shortwave radiation and sea-ice area. (A)** Annual mean incoming top-of-the-atmosphere shortwave radiation at and area within a given latitude. The area within a given latitude band is calculated from simple spherical geometry. The latitudinal dependence of average daily incoming shortwave radiation at the top of the atmosphere is calculated from the very good approximation  $S(\varphi)=1-0.482P_2(\sin(\varphi))$ , where  $P_2$  is the second Legendre polynom (34). **(B)** Same as before, but with x-axis exchanged for clarity.

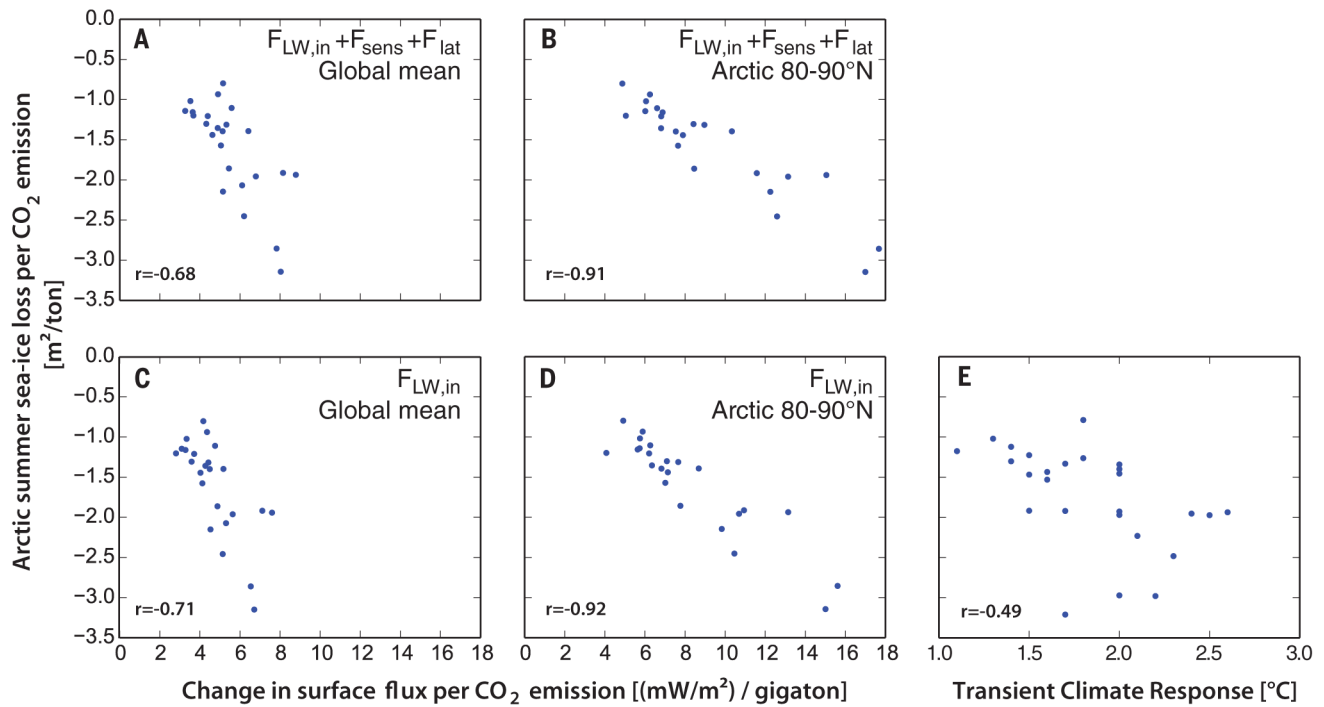


**Fig. 3. Relationship between Arctic sea-ice loss and other metrics.** (A) Each dot represents the sensitivity of Arctic sea-ice loss in a particular model as a function of the increase in global mean incoming nonshortwave fluxes per CO<sub>2</sub> emission in the same model. The latter was obtained from a linear fit of incoming nonshortwave fluxes as a function of cumulative anthropogenic CO<sub>2</sub> emissions during the transition period of each individual model. (B) Same as (A), but fluxes only evaluated in the Arctic. (C and D) Same as (A) and (B), but neglecting sensible and latent heat fluxes. (E) Each dot represents the sensitivity of Arctic sea-ice loss in a particular model as a function of the Transient Climate Response (24) in the same model. (see table S1 for actual values and Supplementary Text for more discussion on panel E). All correlations given in the figure are significant at the 1% level..



## Observed Arctic sea-ice loss directly follows anthropogenic CO<sub>2</sub> emission

Dirk Notz and Julienne Stroeve

published online November 3, 2016

<b>ARTICLE TOOLS</b>	<a href="http://science.sciencemag.org/content/early/2016/11/02/science.aag2345">http://science.sciencemag.org/content/early/2016/11/02/science.aag2345</a>
<b>SUPPLEMENTARY MATERIALS</b>	<a href="http://science.sciencemag.org/content/suppl/2016/11/04/science.aag2345.DC1">http://science.sciencemag.org/content/suppl/2016/11/04/science.aag2345.DC1</a>
<b>RELATED CONTENT</b>	<a href="http://science.sciencemag.org/content/sci/354/6312/533.full">http://science.sciencemag.org/content/sci/354/6312/533.full</a>
<b>REFERENCES</b>	This article cites 32 articles, 2 of which you can access for free <a href="http://science.sciencemag.org/content/early/2016/11/02/science.aag2345#BIBL">http://science.sciencemag.org/content/early/2016/11/02/science.aag2345#BIBL</a>
<b>PERMISSIONS</b>	<a href="http://www.sciencemag.org/help/reprints-and-permissions">http://www.sciencemag.org/help/reprints-and-permissions</a>

Use of this article is subject to the [Terms of Service](#)